View Online / Journal Homepage / Table of Contents for this issue
Dynamic Article Links

Lab on a Chip

Cite this: *Lab Chip*, 2012, **12**, 4178–4184

www.rsc.org/loc

PAPER

Miniaturized platform with on-chip strain sensors for compression testing of arrayed materials†

Luke MacQueen,[a] Oleg Chebotarev,[ab] Craig A. Simmons*[abc] and Yu Sun*[ab]

Received 29th February 2012, Accepted 6th July 2012
DOI: 10.1039/c2lc40670e

Published on 10 August 2012 on http://pubs.rsc.org | doi:10.1039/C2LC40670E
Downloaded by University of Toronto on 08 October 2012

We report a microfabricated mechanical testing platform with on-chip strain sensors for *in situ* mechanical characterization of arrayed materials. The device is based on deformable elastomeric membranes that are actuated by pressure that is delivered through an underlying channel network. The bulging membranes compress material samples that are confined between the membranes and a rigid top-plate. Carbon nanotube-based strain sensors that exhibit strain-dependent electrical resistivity were integrated within the membranes to provide continuous read-out of membrane deflection amplitude. We used this platform to study the cyclic compression of several different silicone samples and thereby measured their elastic moduli. The results obtained using our miniaturized platform were in excellent agreement with those obtained using a commercially available mechanical testing platform and clearly demonstrated the utility of our platform for the mechanical testing of small samples in parallel. The miniaturized platform can significantly increase mechanical testing efficiency, particularly when testing of iterative sample formulations is required.

Introduction

Mechanical testing equipment represents a well-established commercial product sector and is indispensable for quality control and evaluation of new materials. Most testing platforms are limited to serial sample testing and their high costs limit efficient screening of synthetic material formulations. This limitation is especially prohibitive for mechanical testing of polymer blends, biomaterials such as gels and scaffolds, and synthetic biological tissue constructs, all of which require optimization through iterative sample formulations. Structure–property relationships of polymer blends are a major focus of study in materials science.[1]

The mechanical behaviour of structural composites depends on constituent material properties, preparation methods, and strain history. Variations of these properties result in differing composite structural morphologies (*e.g.*, dispersed, stratified, or co-continuous).[2] Blends and composites extend the utilization of many polymers, for example by improving the mechanical properties of natural polymers (*e.g.*, starch, protein and cellulose), synthetic polymers from natural monomers (*e.g.*, polylactic acid) and polymers from microbial fermentation (*e.g.*, polyhydroxybutyrate).[3] Improved mechanical properties of polymer blends are achieved through iterative sample formulation and testing, underscoring a need for increased experimental throughput.

Mechanical testing platforms that test arrayed small-sized samples in parallel have the potential to increase experimental throughput. Although mechanical testing of small samples is achieved using nanoindentation,[4,5] atomic force microscopy,[6,7] and MEMS-based platforms,[8–10] scalable and cost-effective platforms that test millimetre-sized samples are needed to efficiently test "macroscale" bulk properties of materials and to maintain the convenience of using samples that are readily handled by human users without the requirement for additional equipment.

To address the needs for decreased cost and increased throughput of mechanical testing equipment, we developed a miniaturized platform for mechanical compression of arrayed material samples. The operating principle is based on deformable elastomeric membranes that compress samples against a fixed rigid support. Membranes are actuated by pressure supplied through an underlying channel network, and the deflection amplitude is monitored by strain sensors that are integrated in the membranes. We have previously reported a similar platform for cell stretching[11] and biomaterial compression.[12] In our previous work, membrane deflection and biomaterial compression were monitored *ex situ* using confocal microscopy imaging. By integrating highly deformable strain sensors in the membranes, continuous read-out of deflection amplitude is achieved without perturbing the device's operation. We used blended multiwalled carbon nanotubes (MWCNT) and PDMS that

[a]*Department of Mechanical and Industrial Engineering, University of Toronto, 5 King's College Road, Toronto, Ontario, Canada M5S 3G8. E-mail: simmons@mie.utoronto.ca; sun@mie.utoronto.ca; Fax: +1 416 978 7753; Tel: +1 416 946 0548 Tel: +1 416 946 0549*
[b]*Institute of Biomaterials and Biomedical Engineering, University of Toronto, 164 College Street, Toronto, Ontario, Canada M5S 3G9*
[c]*Faculty of Dentistry, University of Toronto, 124 Edward Street, Toronto, Ontario, Canada M5G 1G6*
† Electronic Supplementary Information (ESI) available. See DOI: 10.1039/c2lc40670e

This journal is © The Royal Society of Chemistry 2012

Published on 10 August 2012 on http://pubs.rsc.org | doi:10.1039/C2LC40670E
Downloaded by University of Toronto on 08 October 2012

exhibit strain-dependent electrical conductivity[13,14] to fabricate strain sensors (gauges), as reported previously by others.[15–17]

When samples are confined between the membrane and a rigid support, driving pressure and sample stiffness determine the membrane deflection amplitude that is monitored by the on-chip sensors to measure sample stiffness. To demonstrate the utility of this platform for mechanical compression testing, we used it to cyclically compress silicone elastomers and thereby estimated their elastic moduli, E (0.1–1 MPa). We found excellent agreement between the measurements obtained using our device and a commercially available mechanical testing platform.

Experimental methods

Strain sensors

Multiwalled carbon nanotubes (MWCNT with diameters 20–30 nm and lengths 10–30 μm) were obtained from Cheaptubes Inc. (Cheaptubes, Brattleboro, VT, USA). We blended the MWCNT with PDMS (Sylgard 184, Dow Corning) using various mixing ratios according to a previously reported blend protocol.[14] Briefly: (i) MWCNT and PDMS were dispersed separately in toluene using a 1 : 20 weight ratio for MWCNT and a 1 : 4 volume ratio for PDMS, and stirred magnetically at 50 °C for 2 h; (ii) MWCNT and PDMS solutions were combined and stirred at 50 °C until all the toluene was fully evaporated; (iii) uncured MWCNT–PDMS blends were stored in ambient conditions; (iv) immediately prior to strain sensor fabrication, the PDMS curing agent was added to the blend using a volume ratio of 1 : 10 curing agent to base PDMS polymer. All experiments reported in this work were done using a single batch of MWCNT–PDMS that was blended using 0.91 g MWCNT, 7.0 g PDMS base polymer, and 0.7 g PDMS curing agent.

Strain sensors were "sandwiched" within a PDMS membrane using the procedure outlined in Fig. 1. Thin strips of MWCNT–PDMS were transferred to a PDMS membrane by screen printing and baked at 80 °C for 4 h. The electrical resistivity of the cured blend was $\rho \approx 25$ kΩ·cm. The thickness of the PDMS "substrate" membrane was 50 μm and the MWCNT–PDMS strips had 50 μm thickness, 500 μm width and 1 cm length. After curing the MWCNT–PDMS strips, 100 μm spacers were placed on the PDMS membrane, additional PDMS (also with 1 : 10 curing agent to base polymer) was poured over the surface, and the assembly was squeezed under moderate pressure at 80 °C overnight. The resulting membranes had a total thickness of 150 μm.

Bulging membrane device

Masters for the pressure channels were machined in aluminium, and PDMS was cast on this structure, cured at 80 °C for 4 h, and peeled off. The master was a relief pattern having 8 × 12 cylindrical structures that were connected by channels. The cylindrical structures were of 5 mm diameter, 0.25 mm height, and were spaced by 9 mm centre to centre, conforming to configurations of standard 96-well plates. Channels connecting the cylinders were of 0.25 mm width and 0.25 mm height. For the tests reported here, the 96-element PDMS channel and pressure chamber array was cut into smaller (1 × 4 element) units that were bonded to glass substrates (as shown in Fig. 1C).

Membranes were bonded to the channel layer following exposure of the channel layer and membranes to an oxygen

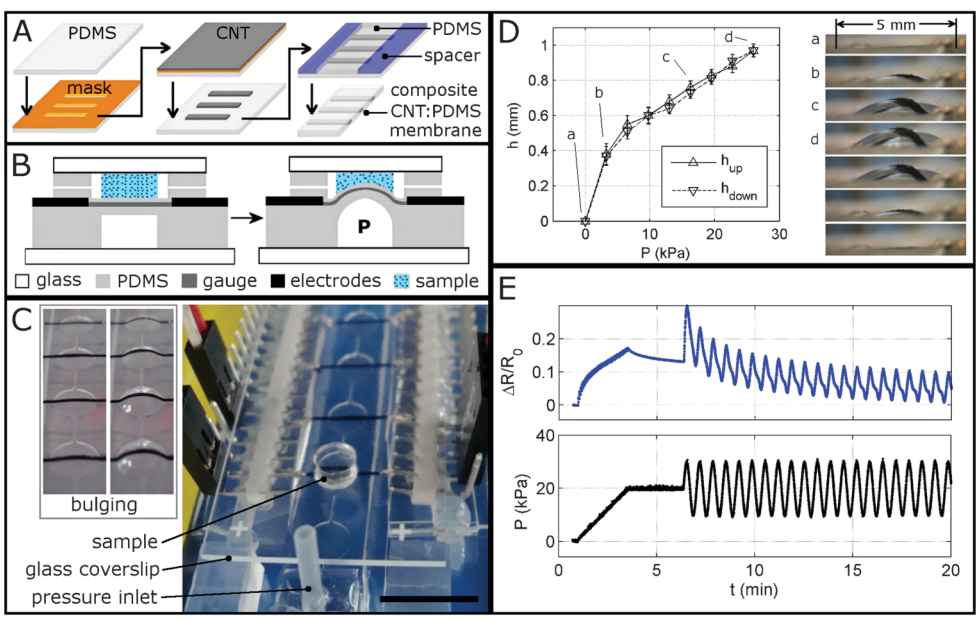

Fig. 1 Micro device array for material mechanical testing. (A) Schematic showing strain sensor fabrication by screen printing thin strips of CNT on PDMS, followed by encapsulation in PDMS (formation of a composite membrane with total thickness = 150 μm); spacers determine the membrane thickness and ensure accessibility of embedded CNT strips for bonding of electrodes; (B) schematic showing sample compression: the sample is confined between the membrane and a glass coverslide supported by spacers; (C) a 4-element device containing a single sample: the inset shows membrane bulging; scale bar = 1 cm; (D) membrane height, h, *versus* pressure, P (data are mean ± SD, $N = 4$); h_{up} and h_{down} refer to h-values that were measured during increasing or decreasing P, respectively; (E) signal of the CNT sensors, $\Delta R/R_0$ (top graph), produced by time-varying pressure application, $P(t)$, shown in the bottom graph.

Published on 10 August 2012 on http://pubs.rsc.org | doi:10.1039/C2LC40670E
Downloaded by University of Toronto on 08 October 2012

plasma (Harrick plasma cleaner model PDC-011, Ithaca, NY). Electrical connectors were bonded to the sensors using a silver conductive epoxy (ρ = 0.02 Ω·cm; MG Chemicals, Toronto, Canada) and DC-resistivity measurements confirmed that the contact resistance was negligible. The strain sensors' electrical resistance was 24.5 ± 5.5 kΩ (mean ± SD, N = 4).

Silicone samples

PDMS samples were prepared by mixing various ratios of curing agent to base polymer (1 : 10, 1 : 20, 1 : 30, and 1 : 40). All silicones were poured into polystyrene dishes and cured at 80 °C overnight. For mechanical tests, cylindrical samples were cut using a hole-punch; their diameters and heights were 5.0 ± 0.5 mm and 3.1 ± 0.1 mm, respectively (N = 4 per composition).

Operation principle and device calibration

A diaphragm pump (Shwarzer, model SP 500EC) and a programmable pressure regulator (Marsh Bellofram, model 3420) were used to deliver pressure, P, into the device channels through a single inlet shown in Fig. 1C. In-house electronics and LabView scripts were used to regulate P and to monitor the strain sensors' electrical resistance. For strain sensing, a fixed voltage of 2.5 V was applied across each sensor and the electrical current was monitored using a precision ammeter (Keithly sourcemeter model 2602). Sensors were preconditioned using a minimum of 4 × 10 min strain runs prior to experiments to ensure reproducible strain signals (Fig. S1†).

During calibration, we measured the height at the centre of each membrane, h, *versus* P, using a Navitar 12× zoom system (Navitar, Rochester, NY) and CCD camera. We measured dh/dP when P was increased or decreased at constant rates (Fig. 1D) and during sinusoidal variation of P (Figs. S2 and S3†). During mechanical testing experiments, we estimated the samples' compressive strain, γ_C = dh/h_{S0}, where h_{S0} is the sample's unstrained height, by comparing measured ($\Delta R/R_0$)/dP and calibrated dh/dP values. A sample's elastic modulus was then estimated to be $E = P/\gamma_C$.

Using a sinusoidal driving pressure (P = 20 ± 10 kPa, f = 0.025 Hz), the maximum height of a freely bulging membrane (without the presence of a material sample) varied with a peak-to-peak amplitude of dh = 0.3 mm (Figs. S2 and S3†). The resistive strain of the sensors was roughly sinusoidal, and the mean value decreased over time (Fig. 1E); following the initial relaxation phase (t ≈30 min), the peak-to-peak amplitude remained constant and its value was $|\Delta R/R_0|$ = 0.08 ± 0.1 (Fig. 2B, Fig. S3†). Under these conditions, we estimated dh/$|\Delta R/R_0|$ = 3.75 ± 0.7 mm, which we used during compression tests to convert $|\Delta R/R_0|$-values to compressive strain, γ_C = dh/h_{S0}, where h_{S0} = 3 mm (*i.e.*, $\gamma_C = 1.25 \times |\Delta R/R_0|$). For the sinusoidal driving pressure, elastic moduli were estimated using full-cycle $\Delta P/\Delta\gamma_C$ values.

For compression testing, our use of a smooth (sinusoidal) time-dependent driving pressure minimized abrupt changes to measured R-values while providing useful ranges of membrane deflection amplitude that permitted characterization of strain

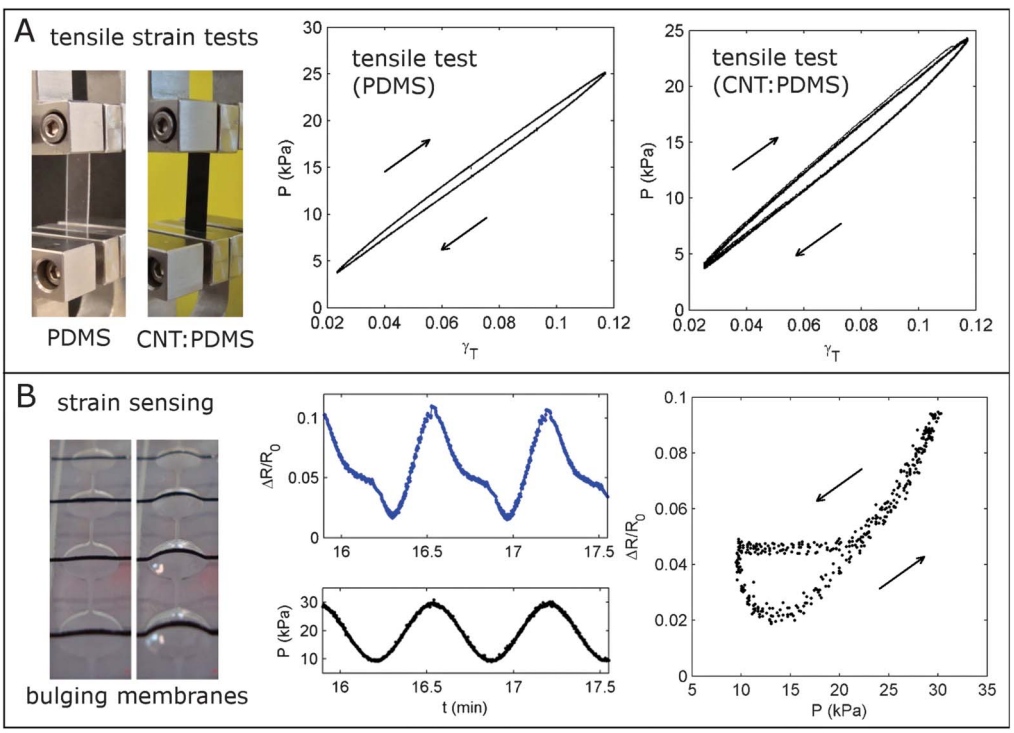

Fig. 2 Tensile properties and resistive strain sensing in CNT–PDMS composite material. (A) Tensile loading of PDMS and CNT–PDMS membranes. (B) Strain sensing during cyclic membrane bulging: the middle panels show the time-dependent resistive strain of the sensors, $\Delta R/R_0$ (top middle panel), and the corresponding input pressure, P (bottom middle panel); this is a selected portion of the data shown in Fig. 1E; the right panel shows the same data as the middle panels plotted as P *vs.* $\Delta R/R_0$.

This journal is © The Royal Society of Chemistry 2012

sensor repeatability over multiple cycles. This loading waveform is shown in Fig. 1E and is described in the following section. We also tested various loading regimes that included ramped, pulsed, or cyclic P. The strain sensors proved to be sensitive to rapid changes in pressure and had a low level of noise. The measured resistance of a typical sensor was $R \approx 25$ kΩ and the error was ~75 Ω (Fig. S4†).

To assess whether the strain sensors and membranes had similar tensile properties, we performed tensile loading tests of CNT–PDMS and PDMS (Fig. 2A) using a commercially available mechanical testing platform (TestResources 840 series), hereafter referred to as the "reference" platform. For these tests, the sample length, width, and thickness were 30 mm, 6.5 mm, and 0.2 mm, respectively, and the cyclic tension was applied using the same reference platform and time-dependent loading profile described above for the compression tests.

Mechanical loading

Mechanical compression of PDMS samples was performed by applying time-dependent pressure (shown in Fig. 1E). First, we slowly ramped the pressure up to P = 20 kPa (dP/dt = 8 kPa min^{-1}), then held it constant for 150 s, and finally applied cyclic P variations (P = 20 ± 10 kPa) at a frequency of f = 0.025 Hz. Identical time-dependent loading conditions were used to compress samples using the reference platform. Sample diameters and heights were 5.0 ± 0.5 mm and 3.1 ± 0.1 mm, respectively (N = 4), for both platforms.

Scanning electron microscopy

We used scanning electron microscopy (SEM) (Hitachi S4000 and S4800) to observe the microscale features of the CNT–PDMS material. A sample having a length, width, and thickness of 10 mm, 5 mm, and 0.2 mm, respectively, was placed on the

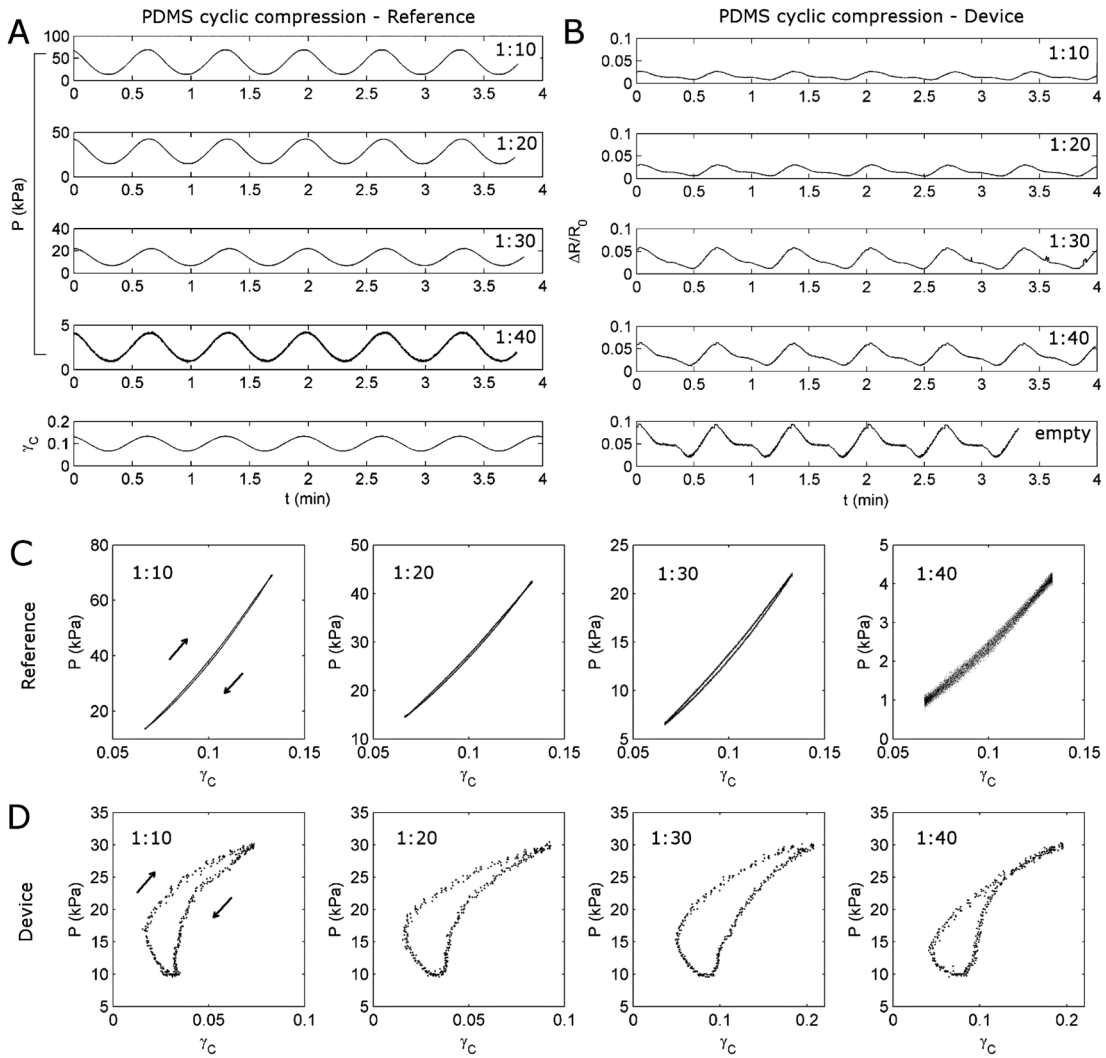

Fig. 3 Cyclic compression of PDMS samples using the reference and microdevice platforms. (A) Sinusoidal driving pressure, $P(t)$, that was required to compress various samples (ratios of curing agent to base polymer are indicated) using the reference platform; the sinusoidal compressive strain, γ_C, that was applied to all samples is shown in the bottom panel (γ_C = 0.1 was the baseline and γ_C = 0.06 was the peak-to-peak sinusoidal amplitude); P clearly decreases for soft samples; (B) resistive strain of the sensors, $\Delta R/R_0$, resulting from a sinusoidal driving pressure when a bulging membrane was empty or contained PDMS samples (ratios of curing agent to base polymer are indicated); (C) plots of P *vs.* γ_C for the plots shown in (A); (D) plots of $\Delta R/R_0$ *vs.* P for the plots shown in (B); arrows in (C) and (D) indicate directions of loading (increasing P) and unloading (decreasing P).

Published on 10 August 2012 on http://pubs.rsc.org | doi:10.1039/C2LC40670E
Downloaded by University of Toronto on 08 October 2012

Published on 10 August 2012 on http://pubs.rsc.org | doi:10.1039/C2LC40670E
Downloaded by University of Toronto on 08 October 2012

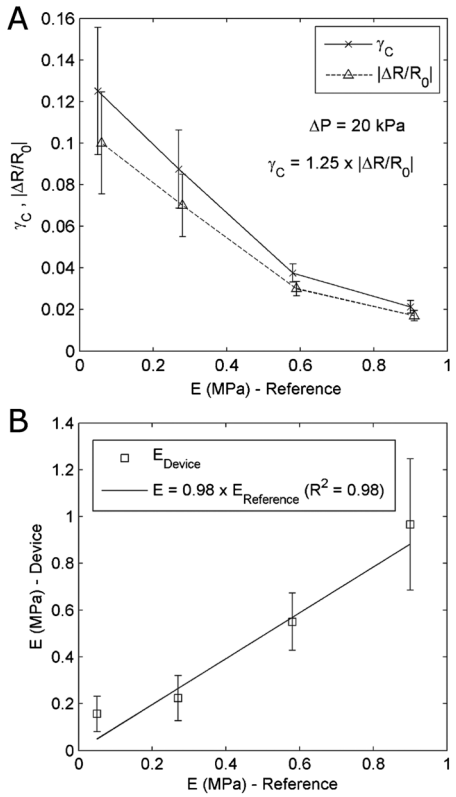

Fig. 4 Measured elastic modulus values. (A) Compressive strain of material samples, γ_C, and resistive strain of the sensors, $\Delta R/R_0$, *versus* compressive modulus values of the samples that were measured using the reference platform; data are shifted slightly on the *E*-axis for clarity; (B) elastic modulus values that were estimated using our microdevice, E_{Device}, *versus* those measured using the calibration platform, $E_{Reference}$; the straight line is a linear best fit of the data and the slope is not significantly different from unity (p = 0.93); data are the mean ± SD (N = 4).

SEM sample holder and electrically grounded using carbon tape. Samples were either unstrained, strained uniaxially by 25%, or were observed 30 min following strain relaxation. Strained samples were manually stretched (length = 12.5 mm) and secured to the sample holder by carbon tape. Their lengths were measured following SEM to ensure that they remained strained during SEM imaging. Measurements were performed under vacuum, and the acceleration voltage used in imaging was 5 kV. In further experiments, we used SEM to observe the cross-section of the embedded strain sensors (Fig. S8†).

Results

The tensile loading behaviour of the PDMS and CNT–PDMS materials was similar although with slightly more hysteresis in the CNT–PDMS sample (Fig. 2A). The tensile elastic modulus of both materials was $E_T \approx 200$ kPa. Strain sensors consisting of thin strips of CNT–PDMS that are embedded in membranes therefore have negligible effects on membrane bulging. The resistive strain of the sensors, $\Delta R/R_0$, clearly depended on the driving pressure that was used to bulge the membranes, although with significant asymmetry between loading and unloading phases (Fig. 2B).

In Fig. 3, we compare cyclic compression of PDMS samples using either the reference or microdevice platforms. Using the reference platform, the pressure required to compress samples decreases for decreasing ratios of curing agent to base polymer (the ratios are indicated in the top-right of each panel in Fig. 3A). Likewise, the resistive strain measured using the microdevice increases for decreasing ratios (Fig. 3B), as a result of increased membrane deflection for soft samples. Loading and unloading regimes were similar using the reference system (Fig. 3C) but were asymmetric using the microdevice (Fig. 3D).

Plots of compressive and resistive strain, γ_C and $|\Delta R/R_0|$, respectively that were obtained during PDMS sample compression tests are shown in Fig. 4A, and the resulting estimated compressive modulus values, $E_{Device} = P/\gamma_C$, are plotted against moduli that were measured using the reference platform ($E_{Reference}$) in Fig. 4B. The range of compressive strain varied ($0.02 < \gamma_C < 0.13$) depending on sample stiffness, as expected, and $\Delta R/R_0$ was directly proportional to γ_C (Fig. 4A). The resulting estimates of E were similar for both platforms (R^2 = 0.98, when device- and reference-data were compared by linear regression; the slope was not significantly different from unity (p = 0.93)).

SEM imaging of CNT–PDMS blends revealed CNT pooling (Fig. 5), indicating that the CNTs were not evenly dispersed in the PDMS. Whether pooling occurred during the blending procedure or during curing is not known and will be the subject of future studies. CNT pools were dispersed randomly in

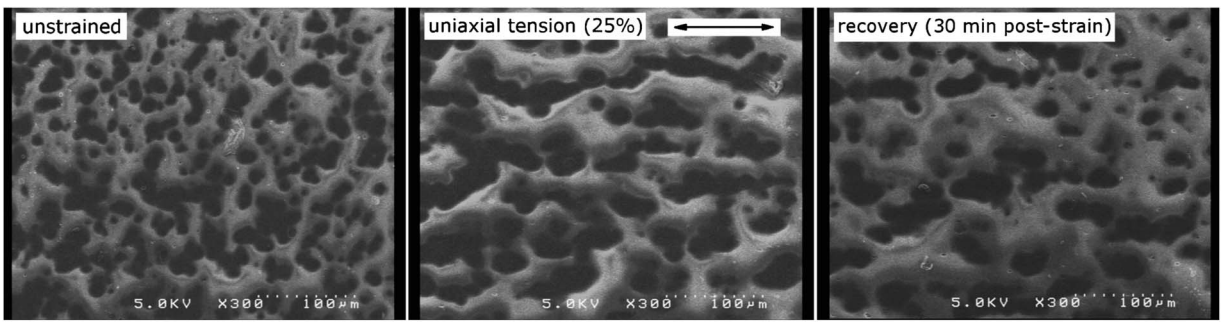

Fig. 5 Scanning electron microscope images of unstrained and strained CNT–PDMS material. Light areas are PDMS and dark areas are high-density CNT clusters (pools) that were randomly distributed in unstrained samples (left panel); uni-axial tension applied to the CNT–PDMS material resulted in coalescence of CNT clusters in the direction of strain (middle panel) and partial recovery was observed 30 min following strain relaxation (right panel).

 This journal is © The Royal Society of Chemistry 2012

Published on 10 August 2012 on http://pubs.rsc.org | doi:10.1039/C2LC40670E
Downloaded by University of Toronto on 08 October 2012

unstrained samples, but they aligned in the direction of strain under uniaxial tension, and only partial recovery of the initially random distribution was observed 30 min following strain relaxation (Fig. 5).

Discussion

We have demonstrated the utility of the miniaturized mechanical testing platform for compression testing of small (mm-scale) silicone samples. The operating principle of our platform is based on bulging elastomeric membranes that have previously been used for microfluidic valves and pumps,[18,19] and for stretching biological cell monolayers.[11,20] In fact, thin film bulging is among the oldest methods used to determine the tensile properties of films (*i.e.*, the so-called "bulge-test"[21–24]). However, the use of bulging membranes to compress samples is a relatively new area of research. Building on our previous work using membranes to compress biomaterials,[12] the integrated strain sensors described here enabled mechanical testing using multiple independent membrane elements without the requirement for *ex situ* observation (*e.g.*, confocal imaging). Fabrication of this platform was simple and scalable, and the number of usable membrane elements that contained strain sensors was limited only by signal acquisition capabilities.

Carbon nanotube-based strain sensors provided a sensitive and reliable readout of membrane deflection amplitude but the loading *vs.* unloading signals were not symmetrical (Fig. 2B, 3D). This asymmetry prevented our use of P/γ_C slopes ($dP/d\gamma_C$) to estimate elastic modulus values (compare Fig. 3C and 3D) that we instead estimated using full-cycle $\Delta P/\Delta\gamma_C$ values. Comparable asymmetry was not observed during tensile loading/unloading of PDMS or CNT–PDMS (Fig. 2A), and it was not observed during sample compression using the reference platform (Fig. 3C). SEM imaging showed the slow recovery of CNT-cluster orientation following strain relaxation (Fig. 5), suggesting that the asymmetry of the measured electrical resistance during loading/unloading can result from the slow recovery of strain-induced nanotube orientation and clustering. Thus, increased electrical resistance resulting from increased inter-nanotube distance during straining was counteracted by pooling of nanotube clusters that tended to align in the direction of strain. Asymmetry in electrical resistivity during loading/unloading has been observed by others using similar MWCNT–PDMS blends[15] and may, therefore, be a general property of this material. Relaxation of the sensor signal (over the time-scale of several minutes) as shown in Fig. 1E also results from strain-induced alignment and coalescence of CNT-rich "pools". When the mean strain value is greater than zero, gradual CNT coalescence lowers the electrical resistivity of the sensor. This hypothesis is supported by Fig. S1† in which sensor conditioning is shown to result in curves that are similar to Fig. 1E. We provide evidence against other potential sources of sensor signal relaxation that include membrane bulge reduction, thermal drift, or delamination of the sensor from its PDMS host material, in Figs. S2, S5, and S8, respectively.† A high-resolution SEM image of a CNT-rich pool showing individual nanotubes is provided in Fig. S9.†

During cyclic compression tests, the strain signal amplitude (peak-to-peak) clearly depended on the sample stiffness (Fig. 3B) and provided excellent estimates of the sample's elastic modulus values (Fig. 4), despite the asymmetry between loading and unloading phases. Although we used a single frequency (f = 0.025 Hz) for our cyclic compression tests, asymmetry of the sensor signal was observed using other frequencies (Fig. S6†), and using saw-tooth waveforms (Fig. S7†). Future work will include dynamic modulus measurements using a range of driving frequencies. Large error bars that are shown in Fig. 4, for samples having large modulus values ($E \approx 1$ MPa, similar to the PDMS that was used to construct the membranes), likely represent a practical limit to the range of E-values that can be measured using this platform (Table 1). To extend this range to higher E samples, fabrication of future platforms may need to make use of materials that are stiffer than PDMS (*e.g.*, for membranes that show improved resistance to sample-induced compression or deformation).

Using blended CNT–PDMS to fabricate our strain sensors, we were able to match the tensile properties of sensors and membranes (Fig. 2A), and the sensors did not perturb the membrane deflection. Furthermore, screen printing of this material is straightforward and can be easily scaled up to larger arrays of membrane elements with arbitrary sensor geometries. The CNT–PDMS material was therefore preferable for this application, compared to thin metallic films[25] or conductive liquids.[26] Our CNT–PDMS material was prepared following the procedure described in ref. 14 and we observed a similar percolation threshold for electrical conductivity (~8 wt%), above which the material had low DC electrical resistivity ($\rho <$ 25 kΩ·cm) that was readily measured using standard equipment. Although the optical transparency of the sensors was not required for our compression tests, applications that require transparent sensors (*e.g.*, for microscopy imaging) require thinner membranes or alternative blending protocols. For example, lower percolation thresholds (1.5 wt%) have been achieved by others using thicker nanotubes (60 nm < outer diameter < 100 nm) and improved CNT dispersion using multiple steps of ultrasonic agitation.[27] Thin transparent CNT layers can also be spray-coated directly onto PDMS surfaces.[16]

Elastic modulus values of PDMS samples that were estimated using the microdevice or reference platforms were similar (Fig. 4B) and demonstrated the utility of our platform for compression testing. We chose PDMS as a model sample material because the range of mechanical properties that resulted from varying the curing agent to prepolymer concentration (0.1 MPa < E < 1 MPa) was representative of a wide range of materials of interest. In addition to the curing agent concentration, PDMS mechanical properties are known to

Table 1 Summary of device properties

Property	Value
$R \pm$ SD (N = 4)/kΩ[a]	24.5 ± 5.5
Resolution ± SD (N = 4)/Ω	75 ± 15
Gauge factor ± SD (N = 4)	1.0 ± 0.13
Membrane area/mm^2	19.6
Maximum load[b]	600 mN, 30 kPa
Load resolution[c]	0.2 mN, 10 Pa
Tested measurement range	Up to 1 MPa

[a] R is the sensor's electrical resistance. [b] Maximum load is determined by driving pressure. [c] Load resolution is determined by electrical resistance resolution.

depend on other preparation conditions that include the curing temperature[28] and time,[29] emphasizing the need for efficient and cost-effective mechanical testing even for this relatively simple polymer. Here, we have shown that our device can be used to test materials with moduli less than ~1 MPa (Table 1) that nevertheless covers a wide variety of polymers. The same operating principle can be used to study stiffer materials although with the requirement of higher driving pressures and possibly the use of different materials to fabricate bulging membranes.

Conclusion

This paper described the development of a miniaturized, on-chip mechanical testing platform and its use for the mechanical compression of PDMS samples. Carbon nanotube-based strain sensors were integrated in deformable membranes. Although the sensors exhibited asymmetrical resistive strain during loading or unloading, they nevertheless provided a reliable indication of the membrane deflection amplitude. Using this platform, we estimated the elastic modulus values of PDMS samples. Agreement with values obtained using a commercially available testing platform demonstrated the utility of our miniaturized platform for mechanical compression testing. The miniaturized mechanical testing platform can be widely applicable for mechanical compression of diverse materials.

Acknowledgements

We thank Robert Ye and Brandon Chen for their assistance with scanning electron microscopy imaging. Funding was provided by the Natural Sciences and Engineering Research Council (NSERC) of Canada (I2IPJ 3962 and RGPIN 327627-06), the Canada Research Chair in Mechanobiology (C.A.S.), and Canada Research Chair in Micro and Nano Engineering Systems (Y.S.).

References

1 *Nano- and Micro-Mechanics of Polymer Blends and Composites*, ed. J. Karger-Kocsis and S. Fakirov, Hanser Publishers, Munich, Germany, 2009.
2 H. Veenstra, P. C. J. Verkooijen, B. J. J. van Lent, J. van Dam, A. P. de Boer and A. P. H. J. Nijhof, *Polymer*, 2000, **41**, 1817–1826.
3 L. Yu, K. Dean and L. Li, *Prog. Polym. Sci.*, 2006, **31**, 576–602.
4 D. M. Ebenstein and L. A. Pruitt, *Nano Today*, 2006, **1**, 26–33.
5 H. Huang, H. Zhao, J. Mi, J. Yang, S. Wan, Z. Yang, J. Yan, Z. Ma and C. Geng, *Rev. Sci. Instrum.*, 2011, **82**, 095101.
6 D. Tranchida, Z. Kiflie, S. Acierno and S. Piccarolo, *Meas. Sci. Technol.*, 2009, 20.
7 Y. Zhu, Z. Dong, U. C. Wejinya, S. Jin and K. Ye, *J. Biomech.*, 2011, **44**, 2356–2361.
8 S. J. Eppell, B. N. Smith, H. Kahn and R. Ballarini, *J. R. Soc. Interface*, 2006, **3**, 117–121.
9 R. Agrawal and H. D. Espinosa, *J. Eng. Mater. Technol.*, 2009, **131**, 041208.
10 K. Kim, J. Cheng, Q. Liu, X. Y. Wu and Y. Sun, *J. Biomed. Mater. Res., A*, 2010, **92**, 103–113.
11 C. Moraes, J. H. Chen, Y. Sun and C. A. Simmons, *Lab Chip*, 2010, **10**, 227–234.
12 C. Moraes, G. Wang, Y. Sun and C. A. Simmons, *Biomaterials*, 2010, **31**, 577–584.
13 M. Park, H. Kim and J. P. Youngblood, *Nanotechnology*, 2008, **19**, 055705.
14 C. X. Liu and J. W. Choi, *J. Micromech. Microeng.*, 2009, **19**, 085019.
15 C. X. Liu and J. W. Choi, *IEEE Trans. Nanotechnol.*, 2010, **9**, 590–595.
16 D. J. Lipomi, M. Vosgueritchian, B. C. K. Tee, S. L. Hellstrom, J. A. Lee, C. H. Fox and Z. N. Bao, *Nat. Nanotechnol.*, 2011, **6**, 788–792.
17 T. Yamada, Y. Hayamizu, Y. Yamamoto, Y. Yomogida, A. Izadi-Najafabadi, D. N. Futaba and K. Hata, *Nat. Nanotechnol.*, 2011, **6**, 296–301.
18 M. A. Unger, H. P. Chou, T. Thorsen, A. Scherer and S. R. Quake, *Science*, 2000, **288**, 113–116.
19 W. H. Grover, A. M. Skelley, C. N. Liu, E. T. Lagally and R. A. Mathies, *Sens. Actuators, B*, 2003, **89**, 315–323.
20 Y. Kamotani, T. Bersano-Begey, N. Kato, Y. C. Tung, D. Huh, J. W. Song and S. Takayama, *Biomaterials*, 2008, **29**, 2646–2655.
21 E. W. Ross and W. Prager, *Q. Appl. Math.*, 1954, **12**, 86–91.
22 T. Tsakalakos, *Thin Solid Films*, 1981, **75**, 293–305.
23 J. J. Vlassak and W. D. Nix, *J. Mater. Res.*, 1992, **7**, 3242–3249.
24 A. L. Thangawng, R. S. Ruoff, M. A. Swartz and M. R. Glucksberg, *Biomed. Microdevices*, 2007, **9**, 587–595.
25 C. S. Li, P. J. Hesketh and G. J. Maclay, *J. Vac. Sci. Technol., A*, 1994, **12**, 813–819.
26 Y. L. Park, C. Majidi, R. Kramer, P. Berard and R. J. Wood, *J. Micromech. Microeng.*, 2010, **20**, 125029.
27 A. Khosla and B. L. Gray, *Mater. Lett.*, 2009, **63**, 1203–1206.
28 M. Liu, J. R. Sun and Q. F. Chen, *Sens. Actuators, A*, 2009, **151**, 42–45.
29 D. Fuard, T. Tzvetkova-Chevolleau, S. Decossas, P. Tracqui and P. Schiavone, *Microelectron. Eng.*, 2008, **85**, 1289–1293.

Published on 10 August 2012 on http://pubs.rsc.org | doi:10.1039/C2LC40670E
Downloaded by University of Toronto on 08 October 2012

This journal is © The Royal Society of Chemistry 2012